Theory of Long-Range Ultracold Atom-Molecule Photoassociation

Jesús Pérez-Ríos,[1,2,*] Maxence Lepers,[2] and Olivier Dulieu[2]
[1]Department of Physics and Astronomy, Purdue University, West Lafayette, Indiana 47907, USA
[2]Laboratoire Aimé Cotton, CNRS/Université Paris-Sud/ENS Cachan, Bâtiment 505, 91405 Orsay, France
(Received 3 May 2015; published 13 August 2015)

The creation of ultracold molecules is currently limited to diatomic species. In this Letter, we present a theoretical description of the photoassociation of ultracold atoms and molecules to create ultracold excited triatomic molecules, thus being a novel example of a light-assisted ultracold chemical reaction. The calculation of the photoassociation rate of an ultracold Cs_2 molecule in its rovibrational ground state with an ultracold Cs atom at frequencies close to its resonant excitation is reported, based on the solution of the quantum dynamics involving the atom-molecule long-range interactions and assuming a model potential for the short-range physics. The rate for the formation of excited Cs_3 molecules is predicted to be comparable with currently observed atom-atom photoassociation rates. We formulate an experimental proposal to observe this process relying on the available techniques of optical lattices and standard photoassociation spectroscopy.

DOI: 10.1103/PhysRevLett.115.073201 PACS numbers: 34.20.-b, 34.50.Cx

Ultracold dilute gases at temperatures much lower than 1 mK offer new opportunities for the study of elementary reactive processes between atoms and molecules. As emphasized in seminal review articles [1,2], this so-called ultracold chemistry is freed from averaging on large velocity distributions. Thus, in this regime the quantum nature of the processes can be accessed, like the presence of resonances or the sensitivity to long-range interactions which can induce anisotropic arrangements prior to the reaction. One of the most advanced experiments in this direction is undoubtedly under progress in JILA at Boulder, where quantum threshold collisions induced by tunneling through a centrifugal barrier between fermionic ultracold KRb molecules have been detected [3,4]. Many experiments demonstrated that conditions suitable for inducing chemical reactions between ultracold ground-state alkali-metal atoms and molecules tightly bound in their electronic ground state are reachable. Ultracold collisions between Cs atoms and Cs_2 [5,6] or LiCs [7] molecules, of Rb and Cs atoms with RbCs molecules [8], or of K and Rb atoms with KRb molecules [9] have been detected through atom trap losses. Three-body recombination and features associated to universal N-body (up to $N = 5$) resonances (like Efimov ones) induced by collisions between atoms and weakly bound molecules have been observed in quantum degenerate gases [10–16].

However, the deep understanding of the collisional dynamics is still to come, as none of these achievements were able to characterize the nature and the state distribution of the final products [17,18]. The heavy mass of alkali-metal species leads to a huge density of resonant states related to the numerous rovibrational levels accessible during an atom-molecule or a molecule-molecule collision, preventing them from being individually characterized. Models connecting the standard treatment of long-range interactions between particles to the presence of numerous resonances mostly resulting from short-range couplings have been developed [18–21] within a statistical framework. The main quantitative uncertainty of such models arises from the estimation of the actual amount of resonant states which are indeed active during the collision.

In this Letter, we propose to use the well-known photoassociation (PA) process to get more insight into such collisions between ultracold atoms and molecules. PA of an ultracold atom pair is a laser-assisted collision creating an electronically excited diatomic molecule often in a weakly bound energy level [22,23]. Under favorable circumstances, such a short-lived molecule can decay by spontaneous emission (SE) into a rovibrational level of a stable electronic state. The PA + SE process played a crucial role in creating samples of stable ultracold molecules [24–27]. This is the simplest example of the formation of a chemical bond under ultracold conditions. The PA step is mostly controlled by long-range atom-atom interactions [28–30], while the SE step involves short-range interaction [24,31]. The knowledge of atom-atom interactions is thus required to fully describe the PA + SE process, which is possible in most cases.

Here we discuss the PA of an ultracold atom with an ultracold diatomic molecule close to the atomic resonant excitation to create ultracold trimers. We evaluate the rate for PA of ultracold ground-state Cs atoms and ultracold ground-state Cs_2 molecules in their lowest rovibrational level, revealing a magnitude similar to the rates observed for atom-atom PA. Our model involves only the long-range interactions between the particles, thus neglecting the influence of the short-range interactions responsible for a possible high density of resonant states addressed in

Refs. [18–21]. Thus, the problem is formally similar to the PA of a pair of atoms of different species. We propose an experimental way to detect the excited Cs_3^* molecules and their possible radiative decay in various products, using an nearly degenerate quantum gas of Cs atoms and molecules trapped in an optical lattice [32]. By comparison to the present simplified model, such an observation would shed light on the role of the short-range physics invoked in Refs. [18–21] in ultracold processes.

We consider the interaction between two charge distributions A and B with total angular momentum $\vec{J}_A$ and $\vec{J}_B$ and separated by a distance R along an axis Z joining their center of mass and oriented from the molecule toward the atom. It can be split according to two distance ranges: (i) the long-range domain where interactions are determined by the individual properties of A and B and can be accurately calculated and (ii) the short-range domain where complex chemical interactions take place. Both domains connect around the LeRoy radius $R_{\rm LR}$ accounting for the size of each distribution [33]. For the rest of the Letter, we consider a $Cs(6\,^2S_{1/2})$ atom and a Cs_2 molecule in the lowest vibrational ($v = 0$) and rotational level $N = 0$ of its electronic ground state $X\,^1\Sigma_g^+$ as the initial state $|i\rangle$ of PA. We have $R_{\rm LR}^i = 42a_0$ ($a_0 = 0.052917721092$ nm). The laser frequency is assumed to be slightly detuned by $\delta_{\rm PA}$ from the $D2$ Cs line, so that PA populates energy levels of the Cs_3^* complex located below the $Cs(6^2P_{3/2}) + Cs_2(X^1\Sigma_g^+, v = 0, N = 0)$ dissociation limit. For these final states, we have $R_{\rm LR}^f = 46a_0$. We ignore the $Cs(6^2P_{3/2})$ hyperfine structure for simplicity, and we will consider experimental conditions where this is a safe approximation.

Following our previous work [34,35], the long-range excited atom-ground-state molecule interaction is treated within the second-order degenerate perturbation theory (see, for instance, [36]). In brief, the Hamiltonian of the system is written as $\hat{H} = \hat{H}_0 + \hat{W}$, where $\hat{H}_0$ refers to the energy of the individual particles at infinity. The atomic states are labeled as $|l = 1, s = 1/2, j, \omega\rangle$, where $j = 1/2, 3/2$ is the total angular momentum quantum number and ω its projection on the Z axis. The molecular states $|X^1\Sigma_g^+, v = 0, N, m_N\rangle$ involve the projection m_N of $\vec{N}$ onto Z. The mutual rotation of the atom and the molecule is not introduced yet, so that the total projection quantum number $\Omega = m_N + \omega$ characterizes the trimer states which will be referred to as $|j, \omega, N, m_N; \Omega; p\rangle$, where $p = (-1)^N$ is the parity. The $\hat{W}(R)$ operator includes the first-order quadrupole-quadrupole term [$\hat{V}_{qq}(R) \propto 1/R^5$, if $N \neq 0$] [37] and the second-order dipole-dipole interaction [$\hat{V}_{dd}^{(2)}(R) \propto 1/R^6$] [38].

The Hamiltonian written in the $|j, \omega, N, m_N; \Omega\rangle$ basis includes the anisotropy of the quadrupole-quadrupole and van der Waals interactions. After diagonalization, it yields the adiabatic potential energy curves (PECs) for large atom-molecule distances displayed in Fig. 1 for $j = 3/2$, $\Omega = 1/2$, and including rotational levels up to $N = 5$.

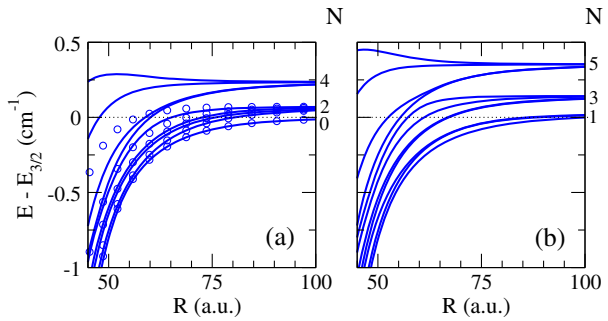

FIG. 1 (color online). Long-range potential energy curves for $\Omega = 1/2$ between a ground-state $Cs_2(X^1\Sigma_g^+, v = 0, N)$ molecule and an excited atom $Cs(6^2P_{3/2})$ as a function of the scattering coordinate R. (a) Even parity; (b) odd parity. The origin of energies is taken at the $Cs_2(X, v = 0, N = 0) + Cs(6^2P_{j=3/2})$ limit. Closed circles in (a) correspond to PECs computed with only $N = 0, 2$ levels included in the Hamiltonian.

The complex structure of the PECs is due to the coupling between the pure electrostatic interaction and the rotation of the molecule. In particular, these PECs cannot be expressed anymore as a pure R^{-n} expansion. For instance, the lowest curve labeled with $N = 0$ at large distance for $j = 3/2, \Omega = 1/2$ (Fig. 1) is more attractive—and thus more favorable for long-range PA—due to the coupling with the $N = 2$ state (see Fig. 2 in Ref. [34]). We also computed the PECs including only $N = 0, 2$ levels in the Hamiltonian, showing that upper rotational levels only slightly affect the lowest PECs for $N = 0$. At $R \approx R_{\rm LR}$ the PECs are attractive by at most 1 cm^{-1}, so that we limit our study to PA detunings smaller than 1 cm^{-1} below the Cs $D2$ line.

In the absence of any spectroscopic information on the trimer PECs, each diagonal term of the above Hamiltonian is smoothly matched for $R < R_{\rm LR}$ to a Lennard-Jones potential $V_{\rm LJ} = D_{\rm LJ}(C_{\rm LJ}/R^6)[(C_{\rm LJ}/R^6) - 1]$. The $C_{\rm LJ}$ factors are chosen equal to the computed C_6 coefficients [38]. For the initial PA state we have $C_6^i = 12101$ a.u. For the final PA states of interest here, namely, with $j = 3/2$, $N = 0, 2$, and $|\Omega| = 1/2$, the values are $C_6^f(N = 0) = 50312$ a.u. and $C_6^f(N = 2) = 18200$ a.u. The depths $D_{\rm LJ}$ are chosen large enough to ensure that the short-range part of the wave functions have a negligible contribution to the ultracold dynamics, following the hypothesis mentioned in the introduction: $D_e^i = 10867.2$ cm^{-1}, $D_e^f(N = 0) = 1500$ cm^{-1}, and $D_e^f(N = 2) = 500$ cm^{-1}. This arbitrarily fixes the relative positions of the energy levels, and thus their couplings and the corresponding PA rates, but does not influence the general findings of the present model.

The radial wave functions $|\Psi_f(\Omega, v')\rangle$ associated to the eigenvalue $E_f(v')$ of the coupled states described by the above PECs are calculated with the mapped Fourier grid Hamiltonian method [39] suitable for calculations at large distances, as the grid step is mapped onto the local kinetic energy of the channels. We used a grid of $N_g = 4145$ points

between $4a_0$ and $7000a_0$ with a scaling parameter $\beta = 0.11$ [39] to ensure a proper convergence of the $E_f(v')$ values.

We assume that PA takes place during an s-wave atom-molecule collision at an energy $E_i = k_B T$, where k_B is the Boltzmann constant and T the related temperature. The associated continuum radial wave function Ψ_i is computed by solving the Schrödinger equation for the entrance channel with the Numerov method. In the perturbative regime, if the PA laser with intensity I_{PA}, detuning δ_{PA}, and polarization $\vec{\epsilon}_{\mathrm{PA}}$ hits a level v' of the Cs_3^* complex, the PA rate is expressed as [28]

$$R_{\mathrm{PA}}(v',T) = A_{if}\left(\frac{3}{2\pi}\right)^{3/2}\frac{h}{2}n_{\mathrm{mol}}\frac{I_{\mathrm{PA}}}{I_0}\Lambda_T^3\Omega_{if}^2|\langle\Psi_i|\Psi_f(\Omega,v')\rangle|^2, \quad (1)$$

where $\Lambda_T = h\sqrt{1/3\mu k_B T}$, μ is the atom-molecule reduced mass, n_{mol} stands for the Cs_2 density, and $A_{if}(\vec{\epsilon}_{\mathrm{PA}})$ is an angular factor depending on $\vec{\epsilon}_{\mathrm{PA}}$. Its value strongly depends on the initial state of the particles, and we took $A_{if} = 1/2$ as a typical example. As the detuning is assumed to be small, the $|i\rangle \rightarrow |f\rangle$ transition dipole moment is taken as the one for the $6^2S_{1/2} \rightarrow 6^2P_{3/2}$ transition, leading to the corresponding atomic Rabi frequency Ω_{if} and saturation intensity $I_0 = 1.1\ \mathrm{mW/cm^2}$ [28]. For the purpose of comparison among various experimental implementations, it is useful to define the normalized PA rate $K_{\mathrm{PA}}(T) = R_{\mathrm{PA}}(T)/n_{\mathrm{mol}}/\phi_{\mathrm{PA}}$ (conveniently expressed in $\mathrm{cm^5}$), where $\phi_{\mathrm{PA}} = I_{\mathrm{PA}}\lambda_{\mathrm{PA}}/hc$ is the PA laser photon flux at the wavelength λ_{PA} [29,40]. The results for $K_{\mathrm{PA}}(T)$ are displayed in Fig. 2(a) for two different temperatures: at $T = 20\ \mu\mathrm{K}$ typical for a magneto-optical trap (MOT), and at $T = 500$ nK representative of a gas close to quantum degeneracy. Like in the case of heteronuclear diatomic molecules [46], the oscillating pattern reflects the strong variations of the spatial overlap between the initial and final radial wave functions with the detuning. As expected from Eq. (1), PA close to quantum degeneracy and for small detunings exhibits a large rate, as already demonstrated in the experiments on Li_2 [45] and Na_2 [44]. We mention that the coupling of the long-range multipolar interactions with the rotational energy quoted above also contributes to enhance the PA rate as the PEC supporting the bound level $|f>$ is more attractive. This first principal result is further illustrated in Fig. 2(b), showing that the predicted PA rate in a MOT environment is comparable to the rates observed with various heteronuclear diatomic species. We recall that the PA rate for Cs_2 at 140 μK [40] was larger than most of the PA rates observed under MOT conditions, as it was enhanced by the presence of a long-range double well in the excited PEC. The large magnitude of the atom-molecule PA rate under quantum degeneracy conditions shows that such an experiment is achievable just like its Li-Li counterpart of Ref. [45].

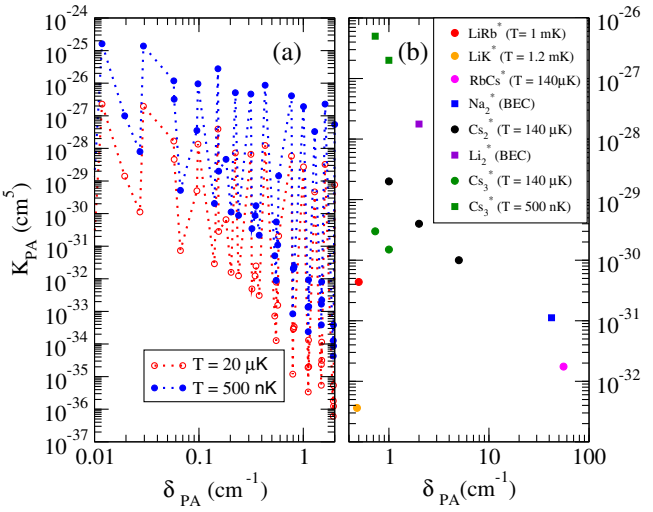

FIG. 2 (color online). (a) Normalized PA rate K_{PA} as a function of the detuning δ_{PA} of the PA laser with respect to $Cs_2(X^1\Sigma_g^+, v = 0, N = 0) + Cs(6^2P_{3/2})$. The points correspond to vibrational levels v' of Cs_3^* for $|\Omega| = 1/2$. The rates are calculated at $T = 20\ \mu$K (open red circles) and $T = 500$ nK (closed blue circles). (b) Comparison of computed K_{PA} values at 140 μK and 500 nK for two Cs_3^* vibrational levels v' at 0.770 and 1.008 $\mathrm{cm^{-1}}$ with the theoretical value in Cs_2 [40], and several experimental rates for LiK [41], LiRb [42], RbCs [43], Na_2 [44], and Li_2 [45].

Although the results look very promising, we must discuss whether the conditions of density and temperature for atoms and molecules needed for the formation of Cs_3^* can be satisfied with the available experimental techniques. A density n_{mol} of $Cs_2(X^1\Sigma_g^+, \nu = 0, N = 0)$ molecules of about $\approx 10^{10}$ to $10^{12}\ \mathrm{cm^{-3}}$ and temperature $T \sim 500$ nK can be obtained by departing from an ultracold sample of ground-state Cs atoms [32] with similar density. These are favorable conditions to initiate a PA experiment where products would be indirectly detected through the loss of molecules.

The direct detection of products is a central objective to better understand the full dynamics of the process, which could benefit from the presence of an optical lattice (OL). The scheme of our experimental proposal is presented in Fig. 3, based on the conditions of Ref. [32]. The motional degrees of freedom of the atoms can be controlled by an OL with wavelength $\lambda_{\mathrm{OL}} = 1064.5$ nm. The OL intensity may be tuned in order to induce a Mott-insulator (MI) state with preferentially two atoms per lattice site (see, e.g., Ref. [47]). The magnetoassociation technique can be employed, creating ground-state Cs_2 molecules in a weakly bound vibrational level. This population can be transferred to the Cs_2 rovibrational ground state by means of stimulated Raman adiabatic passage technique, yielding a molecular MI state to a good approximation [32] [Fig. 3(a)].

During this sequence, a fraction of ultracold atoms could remain unpaired. We propose to tune the OL intensity to

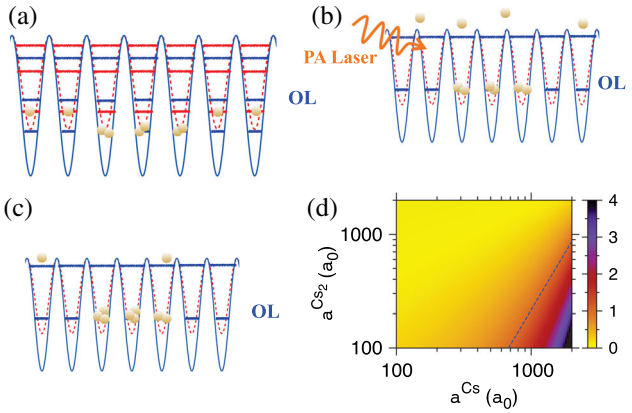

FIG. 3 (color online). Scheme of the experimental proposal. (a) Preparation of a MI state for both atoms and molecules. (b) The PA laser is applied to a mixed molecular MI-atomic SF state. (c) Excited Cs_3^* molecules are created and trapped after radiative decay into stable Cs_3 trimers. (d) Contour plot for the ratio of critical OL intensities for Cs and Cs_2 [Eq. (3)] as a function of their respective scattering lengths. The dashed line indicates where this ratio equals unity.

drive the transition from a MI phase to a superfluid (SF) phase for atoms, keeping the molecules in the MI state [Fig. 3(b)]. Assuming a deep optical lattice with spacing between two successive sites $d = \lambda_{OL}/2$, the MI-to-SF phase transition for the species β ($\beta \equiv$ Cs or Cs_2) would occur when the lattice depth $V_0^\beta \propto \alpha_d^\beta I_{OL}$ (where I_{OL} is the corresponding intensity and α_d^β the dynamic dipole polarizability of the species at λ_{OL}) satisfies the critical value given by [47]

$$\left(\frac{(V_0^\beta)_c}{E_R^\beta}\right) = \frac{1}{4}\ln^2\left(\frac{\sqrt{2}d}{\pi a^\beta}\left(\frac{U^\beta}{J^\beta}\right)_c\right), \tag{2}$$

where E_R^β is the recoil energy of the considered species and a^β is the corresponding scattering length. The critical value $(U^\beta/J^\beta)_c$ of the ratio between the on-site interaction U^β and the tunneling energy J^β depends on the number of β particles per OL sites $\bar{n}$. We will assume $\bar{n} = 1$ hereafter, leading to $(U/J)_c = 29.36$ [47] in the case of a simple cubic lattice. At $\lambda_{OL} = 1064.5$ nm, the recoil energies are such that $E_R^{Cs}/k_B = 64$ nK and $E_R^{Cs_2}/k_B = 32$ nK. Equation (2) shows that the critical value depends on the scattering length a^α of the two species (taken as positive quantities as a MI phase can be achieved) but only through a logarithmic way. While the variations of a^{Cs} are well established [48,49], those of a^{Cs_2} are totally unknown. A reasonable assumption is to consider that the experiment could be performed under conditions where a^{Cs} and a^{Cs_2} are not taking vanishing or infinite values, such that $d/a^\alpha \gg 1$. This leads to the estimation of the ratio of the critical OL intensities for each species

$$\frac{(I_{OL}^{Cs_2})_c}{(I_{OL}^{Cs})_c} \approx \frac{\alpha_d^{Cs} E_R^{Cs_2}}{\alpha_d^{Cs_2} E_R^{Cs}} = \frac{\alpha_d^{Cs}}{2\alpha_d^{Cs_2}}, \tag{3}$$

which must be smaller than unity to ensure that the MI-SF transition is carried out on the atoms without releasing the MI phase of the molecules. Assuming that $\alpha_d^{Cs_2} \approx 2\alpha_d^{Cs}$ [50], the ratio indeed amounts to about 1/4. This estimate is further confirmed in Fig. 3(d), showing that $(I_{OL}^{Cs_2})_c/(I_{OL}^{Cs})_c$ is indeed smaller than unity for a broad range of scattering lengths [Fig. 3(c)] for both species.

The PA laser is not expected to significantly disturb such a hybrid system. Indeed, for $\lambda_{PA} \approx 852$ nm (or $\sim$11737 cm^{-1}, close to the $D2$ Cs line), the Cs_2 ground-state molecule will only weakly absorb such a light due to unfavorable Franck-Condon factors with excited molecular states; hence, the related scattering force will be negligible (see Fig. 3 of Ref. [50]).

Finally, assuming that the photoassociated Cs_3^* complex has a radiative width similar to the one of electronically excited Cs or Cs_2 species, the products of their radiative decay could be discriminated in the experiment [Fig. 3(c)]. On one hand, the radiative decay of Cs_3^* back into three Cs atoms or a Cs/Cs_2 pair with a kinetic energy release will result in a loss of the fragments from the OL. On the other hand, if stable Cs_3 molecules are created after Cs_3^* radiative decay, they will most probably be trapped in the OL, as their recoil energy will be even smaller than the Cs_2 one due to their larger dipole polarizability which induces a deeper trap. A branching ratio between the two decay channels could thus be inferred from the benefit of the "half-collision" character of the PA process leading to bound products.

The observation of ultracold trimers in a PA experiment will shed light on the role of short-range interactions in ultracold collisions as addressed in Refs. [18–21]. Two extreme situations can be envisioned: (i) PA results into well-identified resonant features assigned to Cs_3^* levels determined by pure long-range interactions—as in the present model—suggesting that the coupling with resonances induced by short-range interactions is negligible; (ii) PA reveals a quasicontinuum of Cs_3^* levels induced by the strong coupling of such long-range states with the numerous resonances of the trimer. The presented approach can also be generalized to stable ultracold Cs_2 molecules in their lowest $^3\Sigma_u^+$ state, but this case could be quite challenging, as the PA wavelength will reach the region of numerous Cs_2 excited levels (see Fig. 6 in Ref. [50]). Other combinations can also be investigated with the same method, as only the nature of the long-range interactions will differ from the present case. For instance, the PA of Li atoms and K_2 ground-state molecules would involve a K_2 rotational energy with a similar magnitude than the Li^* spin-orbit splitting, inducing complex patterns in the long-range PECs [35].

The authors acknowledge enlightening discussions with H.-C. Nägerl and K. Lauber in relation with the experimental proposal and W. C. Stwalley for helpful discussions about the PA possibility of $^3\Sigma_u^+$ molecules and ultracold atoms. J. P.-R. acknowledges funding from Institut Francilien de Recherches sur les Atomes Froids (IFRAF) during the development of this project.

*jperezri@purdue.edu

[1] R. V. Krems, Phys. Chem. Chem. Phys. **10**, 4079 (2008).
[2] M. Bell and T. P. Softley, Mol. Phys. **107**, 99 (2009).
[3] K.-K. Ni, S. Ospelkaus, D. Wang, G. Quéméner, B. Neyenhuis, M. H. G. de Miranda, J. L. Bohn, J. Ye, and D. S. Jin, Nature (London) **464**, 1324 (2010).
[4] M. de Miranda, A. Chotia, B. Neyenhuis, D. Wang, G. Quéméner, S. Ospelkaus, J. Bohn, J. Ye, and D. Jin, Nat. Phys. **7**, 502 (2011).
[5] N. Zahzam, T. Vogt, M. Mudrich, D. Comparat, and P. Pillet, Phys. Rev. Lett. **96**, 023202 (2006).
[6] P. Staanum, S. D. Kraft, J. Lange, R. Wester, and M. Weidemüller, Phys. Rev. Lett. **96**, 023201 (2006).
[7] J. Deiglmayr, M. Repp, R. Wester, O. Dulieu, and M. Weidemüller, Phys. Chem. Chem. Phys. **13**, 19101 (2011).
[8] E. R. Hudson, N. B. Gilfoy, S. Kotochigova, J. M. Sage, and D. DeMille, Phys. Rev. Lett. **100**, 203201 (2008).
[9] S. Ospelkaus, K.-K. Ni, D. Wang, M. H. G. de Miranda, B. Neyenhuis, G. Quéméner, P. S. Julienne, J. Bohn, D. S. Jin, and J. Ye, Science **327**, 853 (2010).
[10] T. Kraemer *et al.*, Nature (London) **440**, 315 (2006).
[11] F. Ferlaino, S. Knoop, M. Berninger, W. Harm, J. P. D'Incao, H.-C. Nägerl, and R. Grimm, Phys. Rev. Lett. **102**, 140401 (2009).
[12] M. Zaccanti, B. Deissler, C. DErrico, M. Fattori, M. Jona-Lasinio, S. Müller, G. Roati, M. Inguscio, and G. Modugno, Nat. Phys. **5**, 586 (2009).
[13] S. E. Pollack, D. Dries, and R. G. Hulet, Science **326**, 1683 (2009).
[14] A. Zenesini, B. Huang, M. Berninger, S. Besler, H.-C. Nägerl, F. Ferlaino, R. Grimm, C. H. Greene, and J. von Stecher, New J. Phys. **15**, 043040 (2013).
[15] A. Zenesini, B. Huang, M. Berninger, H.-C. Nägerl, F. Ferlaino, and R. Grimm, Phys. Rev. A **90**, 022704 (2014).
[16] A. Härter, A. Krükow, M. Deiß, B. Drews, E. Tiemann, and J. Hecker Denschlag, Nat. Phys. **9**, 512 (2013).
[17] D. J. Nesbitt, Chem. Rev. **112**, 5062 (2012).
[18] M. González-Martínez, O. Dulieu, P. Larrégaray, and L. Bonnet, Phys. Rev. A **90**, 052716 (2014).
[19] M. Mayle, B. P. Ruzic, and J. L. Bohn, Phys. Rev. A **85**, 062712 (2012).
[20] M. Mayle, G. Quéméner, B. P. Ruzic, and J. L. Bohn, Phys. Rev. A **87**, 012709 (2013).
[21] J. F. E. Croft and J. L. Bohn, Phys. Rev. A **89**, 012714 (2014).
[22] H. R. Thorsheim, J. Weiner, and P. S. Julienne, Phys. Rev. Lett. **58**, 2420 (1987).
[23] K. M. Jones, E. Tiesinga, P. D. Lett, and P. S. Julienne, Rev. Mod. Phys. **78**, 483 (2006).
[24] A. Fioretti, D. Comparat, A. Crubellier, O. Dulieu, F. Masnou-Seeuws, and P. Pillet, Phys. Rev. Lett. **80**, 4402 (1998).
[25] O. Dulieu and C. Gabbanini, Rep. Prog. Phys. **72**, 086401 (2009).
[26] L. D. Carr and J. Ye, New J. Phys. **11**, 055009 (2009).
[27] C. D. Bruzewicz, M. Gustavsson, T. Shimasaki, and D. DeMille, New J. Phys. **16**, 023018 (2014).
[28] P. Pillet, A. Crubellier, A. Bleton, O. Dulieu, P. Nosbaum, I. Mourachko, and F. Masnou-Seeuws, J. Phys. B **30**, 2801 (1997).
[29] R. Côté and A. Dalgarno, Phys. Rev. A **58**, 498 (1998).
[30] J. L. Bohn and P. S. Julienne, Phys. Rev. A **60**, 414 (1999).
[31] C. M. Dion, C. Drag, O. Dulieu, B. L. Tolra, F. Masnou-Seeuws, and P. Pillet, Phys. Rev. Lett. **86**, 2253 (2001).
[32] J. G. Danzl, M. J. Mark, E. Haller, M. Gustavsson, R. Hart, J. Aldegunde, J. M. Hutson, and H.-C. Nägerl, Nat. Phys. **6**, 265 (2010).
[33] R. J. LeRoy, Can. J. Phys. **52**, 246 (1974).
[34] M. Lepers and O. Dulieu, Eur. Phys. J. D **65**, 113 (2011).
[35] M. Lepers and O. Dulieu, Phys. Chem. Chem. Phys. **13**, 19106 (2011).
[36] M.-L. Dubernet and J. M. Hutson, J. Chem. Phys. **101**, 1939 (1994).
[37] M. Lepers, O. Dulieu, and V. Kokoouline, Phys. Rev. A **82**, 042711 (2010).
[38] M. Lepers, R. Vexiau, N. Bouloufa, O. Dulieu, and V. Kokoouline, Phys. Rev. A **83**, 042707 (2011).
[39] V. Kokoouline, O. Dulieu, R. Kosloff, and F. Masnou-Seeuws, J. Chem. Phys. **110**, 9865 (1999).
[40] C. Drag, B. L. Tolra, O. Dulieu, D. Comparat, M. Vatasescu, S. Boussen, S. Guibal, A. Crubellier, and P. Pillet, IEEE J. Quantum Electron. **36**, 1378 (2000).
[41] A. Ridinger, S. Chaudhuri, T. Salez, D. R. Fernandez, N. Bouloufa, O. Dulieu, C. Salomon, and F. Chevy, Europhys. Lett. **96**, 33001 (2011).
[42] S. Dutta, J. Lorenz, A. Altaf, D. S. Elliott, and Y. P. Chen, Phys. Rev. A **89**, 020702 (2014).
[43] A. J. Kerman, J. M. Sage, S. Sainis, T. Bergeman, and D. DeMille, Phys. Rev. Lett. **92**, 033004 (2004).
[44] C. McKenzie *et al.*, Phys. Rev. Lett. **88**, 120403 (2002).
[45] I. D. Prodan, M. Pichler, M. Junker, R. G. Hulet, and J. L. Bohn, Phys. Rev. Lett. **91**, 080402 (2003).
[46] S. Azizi, M. Aymar, and O. Dulieu, Eur. Phys. J. D **31**, 195 (2004).
[47] I. Bloch, J. Dalibard, and W. Zwerger, Rev. Mod. Phys. **80**, 885 (2008).
[48] C. Chin, V. Vuletić, A. J. Kerman, S. Chu, E. Tiesinga, P. J. Leo, and C. J. Williams, Phys. Rev. A **70**, 032701 (2004).
[49] M. Berninger, A. Zenesini, B. Huang, W. Harm, H.-C. Nägerl, F. Ferlaino, R. Grimm, P. S. Julienne, and J. M. Hutson, Phys. Rev. A **87**, 032517 (2013).
[50] R. Vexiau, N. Bouloufa, M. Aymar, J. Danzl, M. Mark, H. C. Nägerl, and O. Dulieu, Eur. Phys. J. D **65**, 243 (2011).